Eur. J. Med. Chem. 36 (2001) 101–108

PII: S0223-5234(01)01214-4/FLA

Point of view

New hypotheses for the GPCR 3D arrangement based on a molecular model of the human sweet-taste receptor

Claude Nofre*

Faculty of Medicine of Lyon Laennec, University of Lyon 1, Lyon, France

Received 16 October 2000; accepted 19 December 2001

Abstract – A molecular model of the human sweet-taste receptor has been inferred from superpositions of 3D maps of sweetener interaction sites (themselves previously deduced from extensive structure–activity relationship studies on highly potent sweeteners) onto three well-known G protein-coupled receptors (GPCRs) — rhodopsin, β_2- and α_{2A}-adrenergic receptors — assumed to be linked by common evolutionary origins. The model gives new answers to old questions on the GPCR 3D structure, such as on the orientation and arrangement of the binding helices, their interaxial distances, radial orientations and relative heights. The model should be useful as a new approach to the rational design of drugs. © 2001 Éditions scientifiques et médicales Elsevier SAS

G protein-coupled receptors / sweet-taste receptors / molecular modelling / drug design

1. Introduction

Sweet stimuli are known to proceed from reversible interactions between sweet-tasting molecules and specific lingual receptors. From indirect evidence [1–3], it is widely accepted today that mammalian sweet-taste receptors are G protein-coupled receptors (GPCRs), although none of them have been convincingly identified to date. Despite the lack of information about the real structure of sweet receptors, it has nevertheless been possible to predict the probable nature and spatial arrangement of several binding sites of the human sweetness receptor (HSR) through extensive structure–activity relationship (SAR) studies [4]. Since it is recognized that GPCRs, which are seven-pass transmembrane receptors (7TMRs), interact with small ligands via the upper half of their three to seven transmembrane α-helical domains (TMs 3–7), an investigation was attempted, on the basis of a possible common evolutionary genetic origin, to determine whether certain TM regions of well-known GPCRs could correspond to or be superposed onto the HSR binding sites inferred previously from SAR studies.

2. Materials and methods

As a consequence of the lack of knowledge on the actual structure of sweet receptors, it has not been possible to apply to the present investigations the usual molecular modelling computational procedures. The paradigmatic bacteriorhodopsin (BR) model was also discarded as a possible 3D template: in fact, since BR — which is a proton pump — is not a GPCR (it is not coupled to a G protein), since there is no characteristic structural homology between BR and GPCRs, since a direct evolutionary link between BR and GPCRs is controversial [5], and since an identical orientation of their TM packing is questionable [6–8], it was considered too hazardous to use BR to design a credible HSR model. Moreover, the real orientation of the GPCR 7TM packing is still unclear. It is generally postulated that GPCR TMs are sequentially oriented anticlockwise when viewed from outside the cell [9], similarly to the BR 3D packing, but it must be noted that the possibility of a clockwise arrangement has not been ruled out to date [10, 11].

* Present address: 114 Cours Albert Thomas, 69008 Lyon, France.
E-mail address: cnofre@worldnet.fr (C. Nofre).

This uncertainty on the actual 3D arrangement of GPCRs led to selecting a modelling approach not exclusively based, as is the rule, on the BR archetype or on the hypothetical 3D pattern of rhodopsin. To construct the present HSR molecular model, a highly pragmatic methodology was adopted, which involved giving priority to the ligand (and not, as usually, to a receptor), and modelling the receptor around the ligands (and not the ligand onto a presumed structure of the receptor), without any a priori assumptions about the 3D arrangement of the receptor. As a result, the methodology chosen constrained me to exclude all automated (or semi-automated) computational techniques, even (and above all) the most sophisticated, and to favour empirical manual approaches in order to conserve complete flexibility and permanent adaptability to the system. The approach was essentially based on the intensive use of the standard CPK atomic models (Harvard Apparatus, Holliston, MA) which were specially conceived for studies on α-helices. More incidentally, and only as a simple complement to the concrete models (which were always preferred to virtual models for our basic investigations), computer-generated models were also used by employing standard molecular geometry parameters.

In order to avoid any possible personal biases or subjective assumptions in the course of the model building and to ensure a maximum of objectivity for the construction of a consistent molecular model, the manually generated model was unceasingly submitted to stringent constraints based on various unequivocal empirical data, such as (i) the need to try and correlate certain of the proposed HSR binding sites with some well-documented interaction sites identified previously in other GPCRs (such as Lys 296 for rhodopsin or Ser 204 for the adrenergic receptors); or (ii) to be able to fit the main natural and artificial sweeteners to the model in order to assess, by cross-validation, the binding sites so inferred.

3. Results and discussion

After multiple attempts, it was found that the HSR binding sites previously suggested from SAR studies [4] can be directly superposed onto several representative residues of the binding domains of three well-defined GPCRs (namely, rhodopsin, β_2-adrenergic receptor, and α_{2A}-adrenergic receptor), with only a few minor changes (four conservative Ser → Thr changes and one nonconservative Phe → Asp change). Among the 16 major binding sites thus inferred, two were arranged in space like two TM3 residues of the human rhodopsin (HRh); five, like five TM4 residues of the β_2-adrenergic receptor ($H\beta_2AR$); five, like five TM5 residues of the human α_{2A}-adrenergic receptor ($H\alpha_{2A}AR$); three, like three TM6 residues of the $H\alpha_{2A}AR$; one, like a TM7 residue of the HRh (*figures* 1 and 2). These 16 binding sites, when denoted according to the Ballesteros–Weinstein integrated numbering system [12], are as follows: T3.33; E3.37; V4.49; V4.52; T4.53; T4.56; T4.57; S5.41; T5.42; C5.43; G5.45; T5.46; D6.52; Y6.55; T6.56; and K7.43 (*figure* 1). Among these sites, 11 (T3.33, E3.37, T4.53, T4.56, T4.57, T5.42, C5.43, T5.46, D6.52, T6.56, and K7.43) are considered as 'key' binding sites (their basic function consists in recognizing natural sweeteners in foods in order to select foods of high nutritional value); five (V4.49, V4.52, S5.41, G5.45, and Y6.55) are regarded as 'accessory' binding sites (they are incidentally involved in the detection of certain artificial sweeteners in association with some key binding sites).

The sequential 3D geometrical arrangement of the α-helices of the modelled HSR, as inferred from docking simulations with numerous artificial or natural sweeteners, is unambiguously clockwise when the bundle of the transmembrane α-helices is viewed from the extracellular side of the cell membrane (*figure* 3a). This inferred orientation is the opposite of the paradigmatic anticlockwise orientation usually advanced for the GPCR α-helix bundles [9] and for the GPCR models which are, as a rule, built either on the BR stereotype as a structural framework [13] (*figure* 3b) or on the alleged anticlockwise 3D arrangement of the rhodopsin helix packing [9].

When the observation is limited to the strictly binding segments (i.e. to the shortest helix portions which bear all the proposed binding sites), the α-helix axes of the modelled binding segments are rigorously parallel, as deduced from numerous HSR/sweetener interaction simulations. Note that it is not necessary to introduce in the model the kinks that the proline residues usually induce in the α-helices; these Pro residues are in fact located out of the docking segments (*figure* 4), and outside or near the borders of the 11-residue truncated portions really used in common practice, whose domain lengths (∼ three turns) are routinely sufficient for studies essentially limited to reception mechanisms.

The modelled HSR helix packing is crescent-shaped (*figure* 5) and is roughly similar (except for the helix bundle orientation) to the rhodopsin arrangement as derived from electron density mapping studies [9, 14–16]. The interaxial distances of the adjacent antiparallel binding helices are ~1.05 nm; of TM3 and TM6, ~1.8 nm; of TM3 and TM7, 1.7 nm. Note the presence, within the TM bundle, of two cavities (denoted A and B): the A cavity (a central cavity which forms a roughly cylindrical pit of ~1 nm in diameter at the core of the five binding TMs) constitutes the binding cavity; the B cavity (a lateral cavity which prolongs the A cavity) is presumed to be a nonbinding cavity and a lateral way for the access of large sweet molecules to the central binding cavity. The radial orientations of the α-helices, as inferred from a simulated interaction with sucrose, are shown in *figure* 6, and their horizontal alignments (relative heights), in *table I*.

From this model, it is moreover possible to infer the presence, in the inactive state of the receptor, of two helix–helix interactions which are assumed to function as two activation switches: one, between E3.37 and K7.43 (*figure* 7a), joins the third and seventh TMs opposite one another through a diagonal link that sweeteners have to split to trigger the activation process of the receptor and elicit a sweet response; the other, between S5.41 and Y6.55 (*figure* 7b), joins the adjacent fifth and sixth TMs through a lateral link whose dissociation is essential to obtain high sweetness potencies from artificial sweeteners.

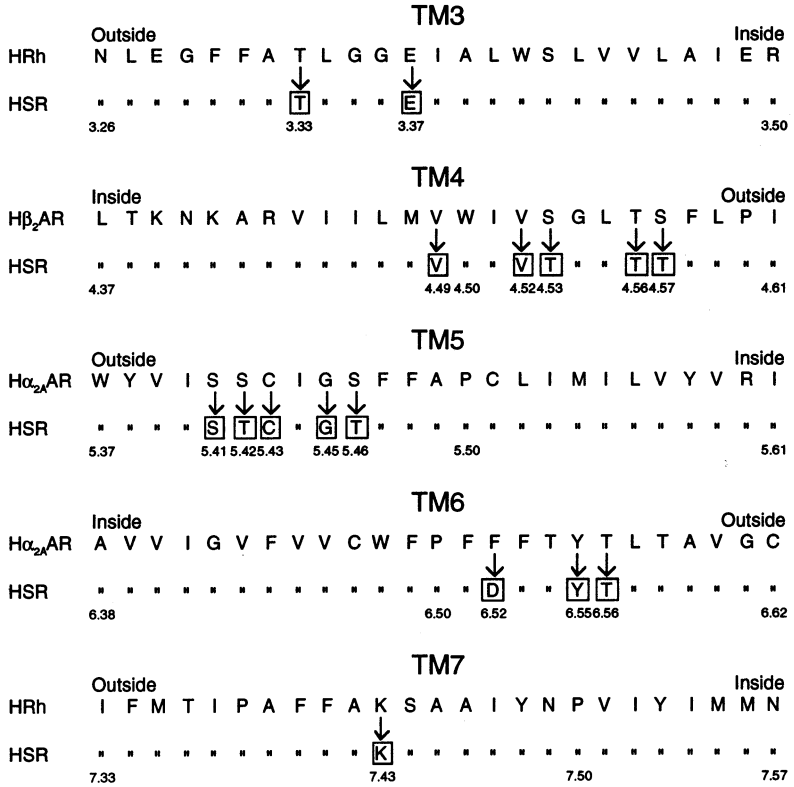

Figure 1. The 16 predicted binding sites (boxed residues) of the HSR as inferred both from extensive SAR data (mainly on high-potency sweeteners) and from superposition studies on the binding domains of three well-characterised GPCRs: TMs 3 and 7 of the human rhodopsin (HRh); TM4 of the human β_2-adrenergic receptor ($H\beta_2AR$); TMs 5 and 6 of the human α_{2A}-adrenergic receptor ($H\alpha_{2A}AR$). Single-letter abbreviations for the amino acid residues are as follows: A, Ala; C, Cys; D, Asp; E, Glu; F, Phe; G, Gly; H, His; I, Ile; K, Lys; L, Leu; M, Met; N, Asn; P, Pro; Q, Gln; R, Arg; S, Ser; T, Thr; V, Val; W, Trp; and Y, Tyr. Residues are identified through their identifier numbers according to the Ballesteros–Weinstein integrated numbering system [12]. 'Outside' refers to the TM part which is near the extracellular face of the cell membrane; 'inside', to the part which is near the intracellular (cytoplasmic) face of the membrane.

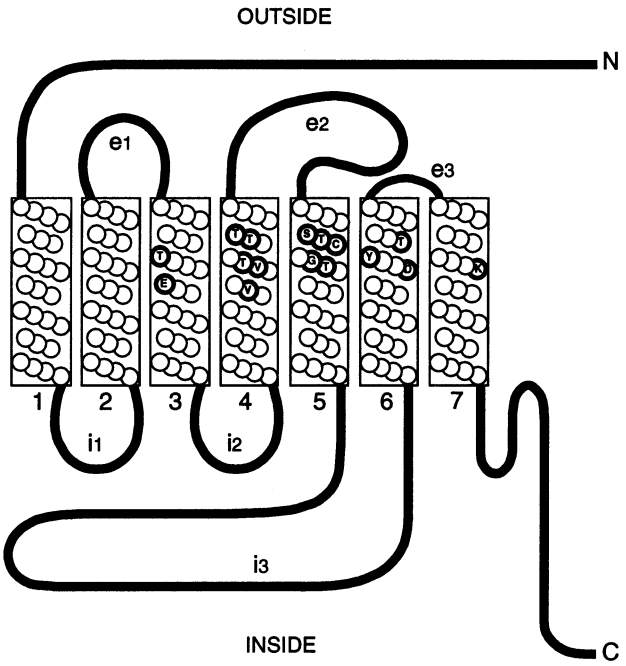

Figure 2. Relative positions of the 16 predicted binding sites (bold circles) of the HSR. Note that the start and end of each helix, at the boundaries of the lipid membrane, are speculative; as the present study is essentially focused on the relative positions of the binding sites, the exact delineations of the α-helices are not useful for the current investigation. N indicates the N-terminus; C, the C-terminus; e1, e2, and e3, the extracellular loops; i1, i2, and i3, the intracellular loops.

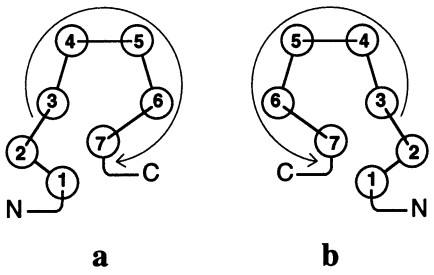

Figure 3. (a) Representation of the proposed clockwise (right-handed) arrangement of the GPCR α-helix packing (as inferred from the present HSR model) when viewed from the extracellular side of the cell membrane; (b) representation of the canonical anticlockwise (left-handed) sequential arrangement of the BR α-helix packing when viewed from the extracellular side.

The functional groups of the 16 predicted binding sites of the HSR operate on sweet ligands through various types of interaction. According to the model,

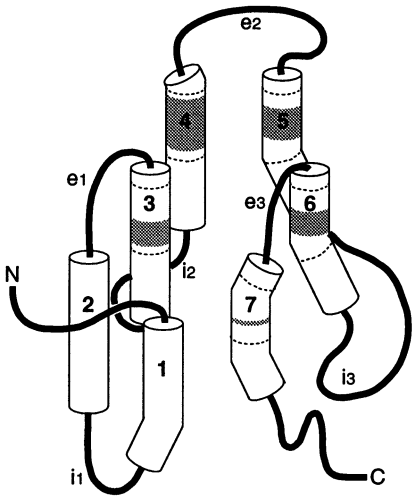

Figure 4. Schematic representation of the HSR model with its kinked TMs owing to the presence of Pro residues (as based on presumed structural homologies between the HSR TMs and TMs 1, 2, 3 and 7 of the HRh, TM4 of the $H\beta_2AR$, and TMs 5 and 6 of the $H\alpha_{2A}AR$). Note that the Pro-induced kinks at positions 4.60, 5.50, 6.50, 7.38 and 7.50 are always out of the strictly binding segments (shaded areas), and outside or near the borders of the 11-residue TM domains (whose limits are indicated by dashed lines) which correspond to the domain lengths used in practice to work with the model.

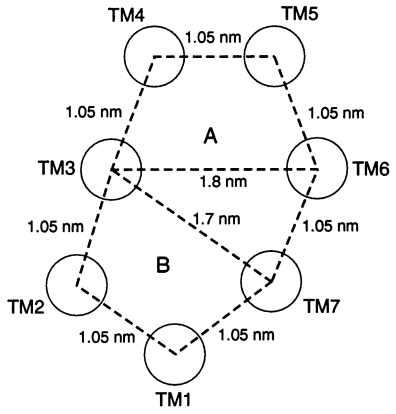

Figure 5. The approximate interaxial distances (nm), according to the model, of the HSR helices as viewed from outside. The positions of the two presumed nonbinding TMs (TM1 and TM2) are speculative and are based only on symmetry considerations. Note the central pit (forming the binding A cavity) at the packing core of the binding domains (TMs 3–7), and, prolonging it downwards, a lateral B cavity, which could be a passage for large sweet ligands.

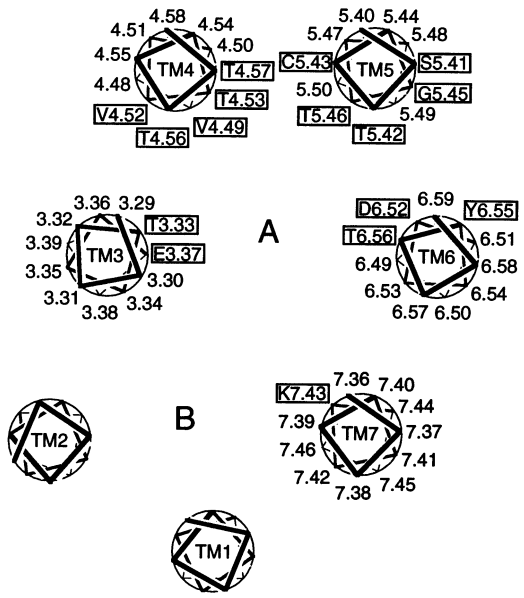

Figure 6. Helical wheel representation, according to the model, of the relative rotational positions of the α-helices when the HSR is viewed from outside; for convenience, the model is limited in the diagram to 11 residues per helix (~ 3 turns). The radial orientations of the five binding helices (TMs 3–7) are derived from a simulated activated state of the receptor by sucrose; note that the radial orientations of the binding helices vary with the nature of the ligands, but that their interaxial distances remain practically constant whatever the ligand. The boxed residues correspond to the 16 predicted binding sites.

Table I. Register (horizontal alignments) of the α-carbons of the binding domains (limited, for convenience, to 11 residues per segment)

TM3	TM4	TM5	TM6	TM7
3.29	4.58	5.40	6.59	7.36
3.30	4.57	5.41	6.58	7.37
3.31	4.56	5.42	6.57	7.38
3.32	4.55	5.43	6.56	7.39
3.33	4.54	5.44	6.55	7.40
3.34	4.53	5.45	6.54	7.41
3.35	4.52	5.46	6.53	7.42
3.36	4.51	5.47	6.52	7.43
3.37	4.50	5.48	6.51	7.44
3.38	4.49	5.49	6.50	7.45
3.39	4.48	5.50	6.49	7.46

Lys (K7.43) works through charge-assisted H-bonding (as a donor) and/or ionic interaction; Asp (D6.52) or Glu (E3.37), through charge-assisted H-bonding (as an acceptor) and/or ionic interaction; Thr (T3.33, 4.53, 4.56, 4.57, 5.42, 5.46, and 6.56), through H-bonding (as a donor and/or an acceptor) and/or steric interaction (often reinforced by steric fits); Cys (C5.43), through H-bonding (mainly as a donor) or steric interaction; Ser (S5.41), through H-bonding (generally as a donor); Tyr (Y6.55), through π–π interaction; Gly (G5.45) and Val (V4.49 and 4.52), through steric interactions (often reinforced by steric fits).

For space reasons, only the interactions of the HSR with the three major natural sweeteners commonly found in foods, namely, D-glucose, D-fructose and sucrose, will be used to illustrate this article (*figure* 8). The interactions with other various natural or synthetic sweeteners will be the subject of forthcoming publications.

For D-glucose (*figure* 8a) (a monosaccharide that is ~ four times less sweet than sucrose on a molar basis), it is known that its heterocyclic oxygen [17, 18] and its anomeric 1-OH [19] are not involved in its interaction with the HSR; moreover, since a tetrol such as D-threitol has the same sweetness potency (~ 0.25 times sucrose on a molar basis) as D-glucopyranose, it follows that D-glucopyranose must similarly interact with the receptor by way of its four alcoholic functions, the 2-, 3-, 4- and 6-hydroxyls. The simulated docking interaction of D-glucopyranose with the receptor model, respecting the above interaction con-

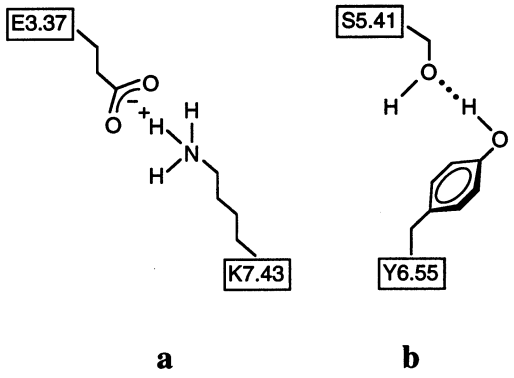

Figure 7. Two major helix–helix interactions of the HSR: (a) a transverse E3.37–K7.43 ionic interaction, whose rupture is assumed to be a prerequisite in triggering the activation of the receptor; (b) a lateral S5.41–Y6.55 H-bonding interaction, which is required to split in order to generate ultrahigh sweet responses — up to 230 000 times the sweetness potency of sucrose with lugduname, the sweetest compound known to date [4].

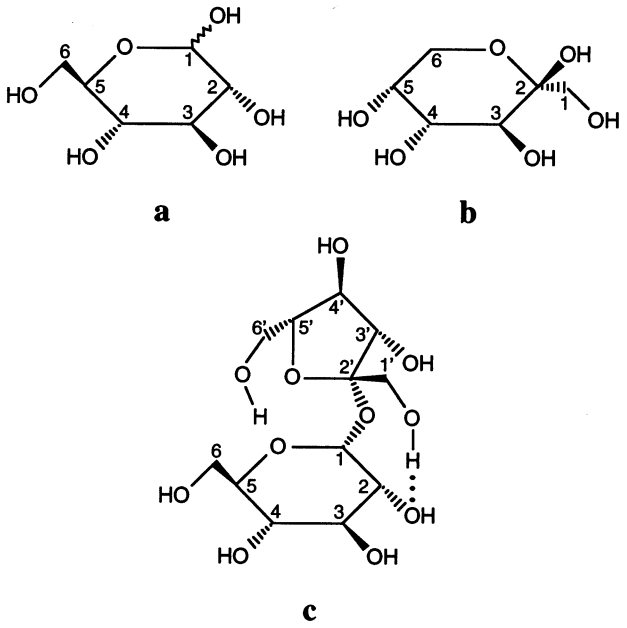

Figure 8. The three major natural ligands of the HSR: (a) D-glucose (D-glucopyranose); (b) D-fructose (β-D-fructopyranose); (c) sucrose (β-D-fructofuranosyl α-D-glucopyranoside). On a molar basis, sucrose is ~two times sweeter than D-fructose, and ~four times sweeter than D-glucose; on a weight basis, sucrose is approximately as sweet as fructose, and ~two times sweeter than D-glucose.

straints and the geometric requirements of a clockwise orientation of the TMs, leads to a simple monomolecular interaction of the ligand with the receptor, by means of the five key binding sites of TMs 3, 6 and 7, via eight H-bonds assisted by two steric interactions (*figure* 9).

For D-fructose (a monosaccharide that is ~two times less sweet than sucrose on a molar basis), which mostly (~73% in the equilibrium isomeric mixture) exists in aqueous solution in the form of β-D-fructopyranose (*figure* 8b), it is known that its heterocyclic oxygen is not implicated in the interaction with the HSR [17, 20]; conversely, its anomeric 2-OH and most of its alcoholic functions appear to be required [21, 22]. The simulated docking interaction of β-D-fructopyranose with the receptor model, when arranged in a clockwise orientation, is consistent with a bimolecular interaction of β-D-fructopyranose with the receptor, one working with the five key binding sites of TMs 3, 6 and 7, via eight H-bonds and two steric interactions, the other, with the six key binding sites of TMs 4 and 5, via five H-bonds and three steric interactions (*figure* 10). Note that the assumption of a bimolecular interaction of D-fructose, as inferred from the simulated interaction, is in agreement with a previous suggestion based on detailed analyses of electrophysiological responses of the gerbil sweetness receptor to various carbohydrates [23]. Finally, the double occupancy of the central binding cavity by D-fructose makes it possible to understand why D-fructose is about two times sweeter than D-glucose on a molar or on a weight basis.

One of the main structural features of sucrose (a disaccharide that is ~two times sweeter than D-fructose and ~four times sweeter than D-glucose on a molar basis, and which may be regarded as the sweetener par excellence) is its ability to retain, in aqueous solution, an intramolecular H-bond between its fructofuranosyl and glucopyranosyl units [24, 25] (*figure* 8c), which gives a semirigid 3D structure to the molecule, making it a unique ligand for studying modelled ligand–GPCR interactions. Out of the various SARs made with sucrose [26, 27], note that its 3-epimer ('*allo*-sucrose') is tasteless [28] and that its 4-epimer ('*galacto*-sucrose') is only slightly sweet [29], which highlights the fundamental importance of the 3- and 4-C configurations of sucrose in triggering the

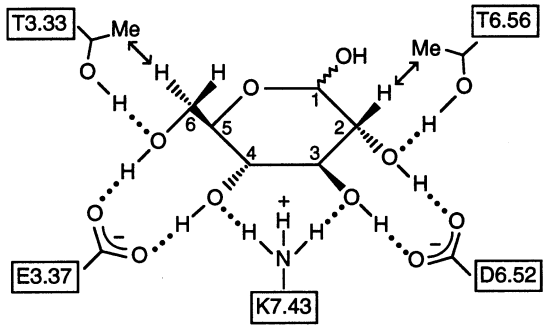

Figure 9. Interaction of D-glucopyranose with the receptor as inferred from a docking simulation with the model (with the TMs arranged in a clockwise orientation). According to the simulation, D-glucopyranose interacts with the receptor through five binding sites of TMs 3, 6 and 7, and via eight H-bonds (represented by dotted lines) and two steric interactions (represented by double-headed arrows). From an energy viewpoint, note that, out of the eight H-bonds involved in the overall interaction, six are charge-assisted (with strongly increased bond energies) and that each alcoholic OH of D-glucopyranose functions both as an H-bond donor group and as an H-bond acceptor group (–H···O–H···), and, as a result, is submitted to cooperative effects [30], with global interaction energies greater than the sum of the individual H-bond energies.

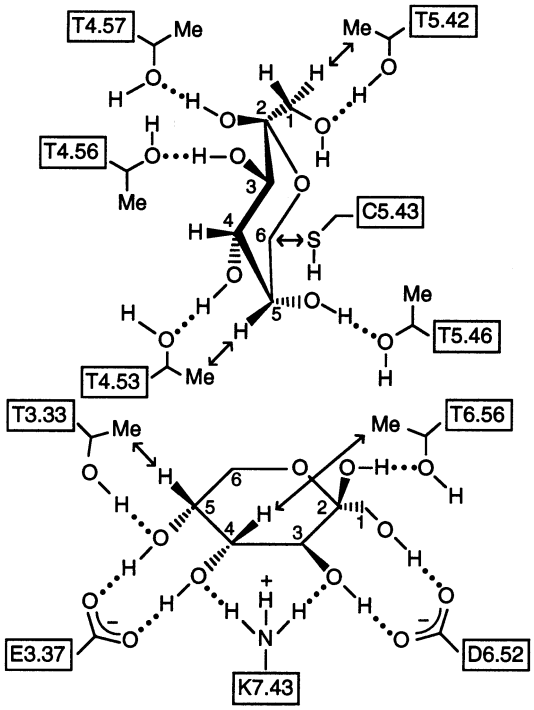

Figure 10. Interaction of β-D-fructopyranose with the receptor as inferred from a docking simulation with the model (with the TMs arranged in a clockwise orientation). According to the simulation, two molecules of β-D-fructopyranose are able to fit onto the receptor (by a double occupancy of the central binding cavity): one, through five binding sites of TMs 3, 6 and 7 and via eight H-bonds and two steric interactions; the other, through six binding sites of TMs 4 and 5 and via five H-bonds and three steric interactions. In total, it is assumed that β-D-fructopyranose interacts with the receptor through 11 binding sites, via 13 H-bonds and five steric interactions. It was also noted that among other docking simulations, xylitol, a pentol, which is 0.35 times sweeter than sucrose on a molar basis, is able, just like D-fructose, to interact with the receptor through a bimolecular interaction by mimicking the 3D structure of β-D-fructopyranose.

activation of the sweet receptor. The simulated docking interaction of sucrose, with the model arranged in a clockwise orientation, shows that the interaction of sucrose is monomolecular, and that (i) the glucopyranosyl moiety interacts through the five key binding sites of TMs 3, 6 and 7 — which delimit the glucopyranosyl (G) binding pocket — via eight H-bonds and two steric interactions; and (ii) the fructofuranosyl moiety, through the six key binding sites of TMs 4 and 5 — which delimit the fructofuranosyl (F) binding pocket — via six H-bonds and four steric interactions. In other words, according to the simulated interaction, sucrose is bound to the receptor by means, in total, of the 11 key binding sites of TMs 3–7, via 14 H-bonds and six steric interactions (*figure* 11).

The model, which was initially developed to design high-potency sweeteners, can also be useful in selecting putative carbohydrate receptors from various taste receptor candidates. Among the mammalian taste receptors proposed so far [31–33], none nevertheless seems to be an evident sweet-taste receptor when compared to the model. However, among the 18 taste receptor candidates recently identified in the fruit fly (*Drosophila melanogaster*) labellum (the major gustatory organ of this insect) [34], the receptor corresponding to the GR23A.1b gene appears to be the probable carbohydrate receptor of this fly when compared to the HSR model; this deduction is based on the presence, in this receptor, of three residues (T125 and E129 in TM3, and K327 in TM7) that are also found in the HSR model as three basic binding sites (T3.33, E3.37, and K7.43, respectively).

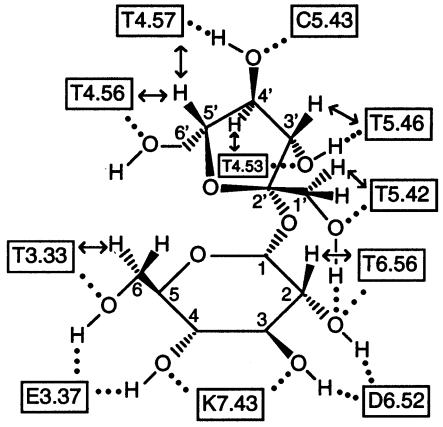

Figure 11. Interaction of sucrose with the receptor as inferred from a docking simulation with the model (with the TMs arranged in a clockwise orientation). According to the simulation, sucrose interacts with the receptor by means (i) of its glucopyranosyl unit through five binding sites of TMs 3, 6 and 7 and via eight H-bonds and two steric interactions; and (ii) of its fructofuranosyl unit through six binding sites of TMs 4 and 5 and via six H-bonds and four steric interactions. In total, it is assumed that sucrose interacts with the receptor through 11 binding sites, via 14 H-bonds and six steric interactions.

4. Conclusions

Finally, the model gives new possible answers to some puzzling questions on the GPCR 3D structure. By putting forward novel clues to the 3D organisation of the GPCR binding domains — such as the clockwise orientation of the binding segments (*figure* 3a), their parallel arrangement (*figure* 4), their interaxial distances (*figure* 5), their radial orientations (*figure* 6), and their relative heights (*table I*) — the model provides new challenging concepts for the prediction of the GPCR 3D structure, new leads for site-directed mutagenesis, new views on the ligand binding modes, and a new approach to the rational design of ligands.

Acknowledgements

I thank J.-M. Tinti for helpful discussions, and E. Le Bredonchel for technical assistance.

References

[1] Kinnamon S.C., Margolskee R.F., Curr. Opin. Neurobiol. 6 (1996) 506–513.

[2] Lindemann B., Physiol. Rev. 76 (1996) 719–766.

[3] Naim M., Striem B.J., Tal M., Adv. Food Nutr. Res. 42 (1998) 211–243.

[4] Nofre C., Tinti J.-M., Food Chem. 56 (1996) 263–274.

[5] Soppa J., FEBS Letters 342 (1994) 7–11.

[6] Kontoyianni M., DeWeese C., Penzotti J.E., Lybrand T.P., J. Med. Chem. 39 (1996) 4406–4420.

[7] Rippmann F., in: Findlay J.B.C. (Ed.), Membrane Protein Models, Bios Scientific, Oxford, 1996, pp. 91–104.

[8] Thomas P., in: Findlay J.B.C. (Ed.), Membrane Protein Models, Bios Scientific, Oxford, 1996, pp. 73–89.

[9] Baldwin J.M., EMBO J. 12 (1993) 1693–1703.

[10] Lybrand T.P., in: Findlay J.B.C. (Ed.), Membrane Protein Models, Bios Scientific, Oxford, 1996, pp. 145–159.

[11] Pardo L., Batlle M., Duñach M., Weinstein H., J. Biomed. Sci. 3 (1996) 98–107.

[12] Ballesteros J.A., Weinstein H., in: Sealfon S.C. (Ed.), Methods in Neurosciences, vol. 25, Academic, San Diego, 1995, pp. 366–428.

[13] Henderson R., Baldwin J.M., Ceska T.A., Zemlin F., Beckman E., Downing K.H., J. Mol. Biol. 213 (1990) 899–929.

[14] Schertler G.F.X., Villa C., Henderson R., Nature 362 (1993) 770–772.

[15] Unger V.M., Hargrave P.A., Baldwin J.M., Schertler G.F.X., Nature 389 (1997) 203–206.

[16] Krebs A., Villa C., Edwards P.C., Schertler G.F.X., J. Mol. Biol. 282 (1998) 991–1003.

[17] Lindley M.G., Shallenberger R.S., Whistler R.L., J. Food Sci. 41 (1976) 575–577.

[18] Suami T., Ogawa S., Toyokuni T., Chem. Lett. (1983) 611–612.

[19] Birch G.G., Shamil S., Shepherd Z., Experientia 42 (1986) 1232–1234.

[20] Ogawa S., Uematsu Y., Yoshida S., Sasaki N., Suami T., J. Carbohydr. Chem. 6 (1987) 471–478.

[21] Lindley M.G., Birch G.G., J. Sci. Food Agric. 26 (1975) 117–124.

[22] Szarek W.A., Rafka R.J., Yang T.-F., Martin O.R., Can. J. Chem. 73 (1995) 1639–1644.

[23] Jakinovich W., Goldstein I.J., Brain Res. 110 (1976) 491–504.

[24] Bock K., Lemieux R.U., Carbohydr. Res. 100 (1982) 63–74.

[25] McCain D.C., Markley J.L., Carbohydr. Res. 152 (1986) 73–80.

[26] Lichtenthaler F.W., Immel S., in: Mathlouthi M., Kanters J.A., Birch G.G. (Eds.), Sweet-Taste Chemoreception, Elsevier, London, 1993, pp. 21–53.

[27] Hough L., Khan R., in: Mathlouthi M., Kanters J.A., Birch G.G. (Eds.), Sweet-Taste Chemoreception, Elsevier, London, 1993, pp. 91–102.

[28] Hough L., O'Brien E., Carbohydr. Res. 84 (1980) 95–102.

[29] Lindley M.G., Birch G.G., Khan R., J. Sci. Food Agric. 27 (1976) 140–144.

[30] Jeffrey G.A., Saenger W., Hydrogen Bonding in Biological Structures, Springer-Verlag, Berlin, 1994.

[31] Abe K., Kusakabe Y., Tanemura K., Emori Y., Arai S., J. Biol. Chem. 268 (1993) 12033–12039.

[32] Hoon M.A., Adler E., Lindemeier J., Battery J.F., Ryba N.J.P., Zuker C.S., Cell 96 (1999) 541–551.

[33] Matsunami H., Montmayeur J.-P., Buck L.B., Nature 404 (2000) 601–604.

[34] Clyne P.J., Warr C.G., Carlson J.R., Science 287 (2000) 1830–1834.